

---

## ORIENTATION OF HIGH-RESOLUTION SATELLITE IMAGES BASED ON AFFINE PROJECTION

Susumu Hattori, Tetsu Ono\*, Clive Fraser\*\* and Hiroyuki Hasegawa\*\*\*

Fukuyama University, Japan, Dept. of Computer Science  
hattori@fuip.fukuyama-u.ac.jp

\*Kyoto University, Japan, Dept. of Global Engineering  
ono@jf.gee.kyoto-u.ac.jp

\*\*Melbourne University, Australia, Dept. of Geomatics  
c.fraser@eng.unimelb.edu.au

\*\*\*Geonet Inc., Japan  
hasegawa@geonetz.com

**KEY WORDS:** Satellite images, affine projection, sensor orientation, SPOT, MOMS-2P

### ABSTRACT

This paper discusses an orientation method for high-resolution satellite images based on the affine projection model. The conventional central projection model can lead to over-parameterisation due to the narrow field of view of the optics, which in turn can cause instability in the orientation. It is shown that the affine model offers a solution to this problem since it can absorb linear distortions in orientation parameters while at the same time stabilising the orientation/triangulation process. The assumption is made with the affine model that the satellite travels in a straight path at uniform velocity within the model space, where the chosen datum is the Gauss-Krueger projection (or UTM). The affine model has been validated through experiments conducted with both SPOT and MOMS-2P stereo imagery, and the results of practical tests are reported. These show that the affine approach, which needs no prior knowledge of sensor trajectory or a precise camera model, can yield sub-pixel ground point triangulation accuracies, while displaying a high level of solution stability.

### 1 INTRODUCTION

High-resolution satellite imaging sensors feature very long focal lengths and narrow fields of view. This imaging geometry can lead to over-parameterisation in orientation/triangulation if the conventional central projection model is adopted for restitution. The problem becomes more acute as the field of view narrows. If sensor interior orientation is known, and high precision navigation sensors are available to provide position and attitude data for the satellite line scanner, either all or some of the exterior orientation parameters can be constrained to suppress over-parameterisation and thus stabilise the orientation/triangulation process. As an alternative restitution approach, a model based on affine projection can be considered. The late Professor Okamoto proposed such an approach (Okamoto, 1981,1988; Okamoto & Akamatsu, 1992a;b) and over recent years efforts have been made to investigate the geometric and algebraic properties of affine projection, and to formulate and evaluate alternative sensor orientation and triangulation models for satellite line scanner imagery (Okamoto et al.,1998;1999).

The present paper integrates the theories and procedures of affine-based orientation for satellite line scanner imagery and shows through experimental results that the method can produce a precise and stable algorithm for exterior orientation of satellite imagery. Moreover, the affine model exhibits some advantages over conventional central projection approaches and these become more pronounced with narrower fields of view of the sensor. The reported experiments utilised stereo images of SPOT and MOMS-2P, where ground control points (GCPs) and check points were recorded to sub-metre accuracy by aerial photogrammetry and GPS surveying.

### 2 CATEGORIES OF ORIENTATION METHODS

The imaging systems of high-resolution satellites are typically linear, push-broom scanners. Orientation methods developed to date for satellite imagery, typically SPOT images, may be classified into two groups. The first involves the formulation of a strict central projection model, with the trajectory and orientation of the satellite sensor being described in a 3D Cartesian coordinate system (Kratky, 1989; Gagan, 1988; Westin, 1990; Trinder, 1988). The second approach involves the formulation of a projection model which simulates conventional stereo photogrammetric restitution for frame imagery, using collinearity equations. With this method, restitution

of satellite line scanner imagery can be carried out on standard digital photogrammetric workstations using traditional models with minor modifications (eg Konecny et al., 1987; Kruck & Lohmann, 1986; Kruck, 1988).

In some respects, the affine model to be discussed can be regarded as an expansion of that proposed by Kruck (1988), which utilised the Gauss Krueger projection plane and ellipsoidal heights as a reference coordinate system. This system will be referred to as 3D-GK in the following discussion. Orientation angles forming the collinearity equation can then be fixed as constant by assuming the satellite travels linearly in the object space, at constant velocity. This assumption enables parameter suppression to avoid instability in the orientation/triangulation. For compensation of non-linear fluctuations of parameters, which cannot be accounted for, eight additional parameters are added to the collinearity model. These comprise the distortion correction for Earth rotation, along with perturbation terms for interior and exterior orientation parameters.

### 3 MATHEMATICAL MODELS OF AFFINE PROJECTION

A line-scanner image constitutes a 2D central perspective projection. The conventional central projection equation (collinearity equation) relating image coordinates  $u, v$  with object space coordinates  $X, Y, Z$  therefore needs to be modified for push-broom scanner imagery to:

$$\begin{aligned} 0 &= a_{11}(X - X_0) + a_{12}(Y - Y_0) + a_{13}(Z - Z_0) \\ v &= \frac{a_{21}(X - X_0) + a_{22}(Y - Y_0) + a_{23}(Z - Z_0)}{a_{31}(X - X_0) + a_{32}(Y - Y_0) + a_{33}(Z - Z_0)} \end{aligned} \quad (1)$$

where  $X_0, Y_0, Z_0$  are the coordinates of the projection center;  $u$  and  $v$  are in the flight direction and sensor direction, respectively;  $c$  is the focal length; and  $a_{ij}$  are the elements of the rotation matrix  $\mathbf{A}$ . It is noteworthy that the  $u$  coordinate is always zero. The exterior orientation parameters, which are unique for each scan line, are modelled as continuous functions of time or line number, usually by low-order polynomials.

Okamoto (1988) modified Eqs.1 to the form of general projective equations, Eqs.2, in order to effect corrections for linear distortions within the parameters:

$$\begin{aligned} 0 &= X + A_1Y + A_2Z + A_3 \\ v &= \frac{A_4Y + A_5Z + A_6}{A_7Y + A_8Z + 1} \end{aligned} \quad (2)$$

Eqs. 2, in which the coefficients  $A_i$  are again modelled as functions of time or line number, will be referred to here as the *1D Perspective Model*. In order to avoid over-parameterisation in instances where the sensor view angle is very narrow (eg less than 1 degree for the new generation of 1m satellites such as Ikonos), an affine projection model can substitute for the expression for the in-line sensor coordinate  $v$ :

$$\begin{aligned} 0 &= X + A_1Y + A_2Z + A_3 \\ v &= A_4Y + A_5Z + A_6 \end{aligned} \quad (3)$$

The model represented by Eqs.3 is here termed a *1D affine model*, in which the coefficients are again described by functions of time. In Eqs.1 through Eqs.3, the object space coordinate system is assumed as 3D Cartesian. As will be suggested in the following, however, the latter two models are also applicable for the 3D-GK coordinate system, so long as a height correction for Earth curvature is applied.

With regard to the time-dependent modelling of the coefficients  $A_i$ , these parameters are expected to be constant or at least piecewise linear within the relatively small extent of a single satellite image scene. For the reported experiments, a linear variation model (Hoffmann, 1986) has been applied, which means that every parameter introduces two unknowns into the resulting least-squares model for orientation/triangulation.

Okamoto et al. (1996, 1999) further extended Eqs.2 and 3 to the following two projection models:

$$\begin{aligned} u &= B_1X + B_2Y + B_3Z + B_4 \\ v &= \frac{B_5X + B_6Y + B_7Z + B_8}{B_9X + B_{10}Y + B_{11}Z + 1} \end{aligned} \quad (4)$$

$$\begin{aligned} u &= B_1X + B_2Y + B_3Z + B_4 \\ v &= B_5X + B_6Y + B_7Z + B_8 \end{aligned} \quad (5)$$

The first of these, Eqs. 4, is termed the *Parallel Perspective Model*, whereas the second, Eqs. 5, will be referred to as the *2D Affine Model*. It is noteworthy that in neither of these models are the parameters modelled as

time-variant functions. Instead, a single coefficient value relates to all scan lines in the orientation process, which implies that the following conditions are met: Firstly, the satellite moves in space linearly and at uniform velocity with constant orientation parameters. This supports use of the 3D-GK as the object space coordinate system, as in Kruck (1988), whose model is very similar to Eqs. 4 except that the parameters  $B_i$  there constitute elements of a rotation matrix. This first condition is reasonable for near-nadir pointing sensors where variation in terrain height is modest, but it is not so suitable in high-latitude areas. The second condition is that the collinearity equation holds between image coordinates and object space coordinates, which is fulfilled when utilising the 3D-GK through application of an Earth curvature correction.

The 2D affine model (Eqs.5) strictly only holds if the field view is infinitesimally small, which is clearly not the case in practise. The difficulty of applying this model to satellite line scanners with fields of view of a few degrees or more (eg  $4^\circ$  for SPOT) is overcome by an initial transformation of the 2D perspective image to an affine projection, a process that will be further discussed in the following section.

Eqs.4 and 5 form a solid model in space just as with conventional stereo frame imagery. In order to absolutely orient the model in object space, the number of GCPs required for the parallel perspective and 2D affine models are five and four, respectively. To illustrate this, we let the space be reconstructed from a pair of stereo photographs in which image and object space coordinates are related by general projective equations:

$$\begin{aligned} u &= \frac{B_1X + B_2Y + B_3Z + B_4}{B_9X + B_{10}Y + B_{11}Z + 1} \\ v &= \frac{B_5X + B_6Y + B_7Z + B_8}{B_9X + B_{10}Y + B_{11}Z + 1} \end{aligned} \quad (6)$$

The model space coordinates  $X_m, Y_m, Z_m$  and object space coordinates  $X, Y, Z$  are related by linear transformation of a homogenous coordinate system of fourth degree:

$$\begin{pmatrix} X_m \\ Y_m \\ Z_m \\ t \end{pmatrix} = \begin{pmatrix} C_1 & C_2 & C_3 & C_4 \\ C_5 & C_6 & C_7 & C_8 \\ C_9 & C_{10} & C_{11} & C_{12} \\ C_{13} & C_{14} & C_{15} & 1 \end{pmatrix} \begin{pmatrix} X \\ Y \\ Z \\ T \end{pmatrix} \quad (7)$$

Since the coefficients  $C_i$  are determined by five GCPs, the rank of the observation equations formed by the coplanarity condition is at best 7 (22-15). The case of Eqs.4 is the same and accordingly the equivalence to Eq.7 for the 2D affine model is

$$\begin{pmatrix} X_m \\ Y_m \\ Z_m \end{pmatrix} = \begin{pmatrix} D_1 & D_2 & D_3 \\ D_4 & D_5 & D_6 \\ D_7 & D_8 & D_9 \end{pmatrix} \begin{pmatrix} X \\ Y \\ Z \end{pmatrix} + \begin{pmatrix} D_{10} \\ D_{11} \\ D_{12} \end{pmatrix} \quad (8)$$

More than four GCPs are thus necessary to determine the 12 unknowns, and the rank of the observation equations via the coplanarity condition is  $16-12 = 4$ .

#### 4 TRANSFORMATION: CENTRAL PERSPECTIVE TO AFFINE PROJECTION

Considering that the field of view of SPOT is four degrees, the projection of a SPOT image effectively stands between central perspective and affine. Errors due to discrepancies in projection when applying the affine model can be eliminated by a transformation of images from central perspective to affine projection (Okamoto & Akamatsu, 1992a;b). This procedure, however, requires a knowledge of terrain height, which is invariably unavailable for the area covered by the imagery. The contradiction is overcome by a straightforward iterative procedure of stereo measurement. For the discussion of the image transformation, the following symbols are used:  $v$  is the pixel coordinate in the central projection image,  $v_a$  is the corresponding coordinate in the affine projection image,  $c$  is the focal length,  $p_H$  is the principal point and  $2\alpha$  is the field view angle.

4.1 Case of Flat Terrain

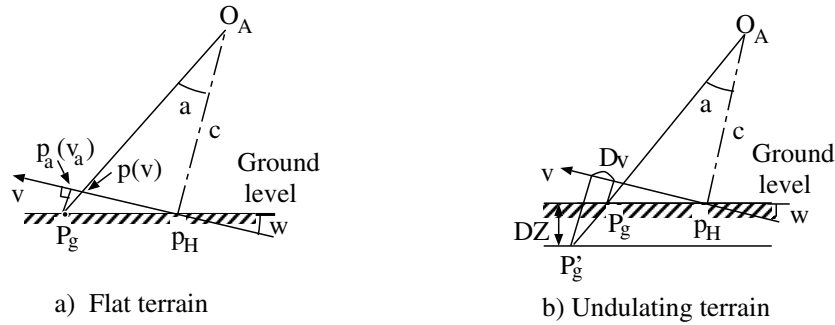


Figure 1: Image transformation from central perspective to affine projection

Let us first assume that the terrain is flat and approximate height is known. Fig.1a depicts the case with unit scale. The line scanner image intersects the ground at the principal point. Point  $p(v)$  in the central projection image is transformed to  $p_a(v_a)$  in the affine projection via ground point  $P_g$  and according to Eq.9.

$$v_a = \frac{v}{1 - v \tan \omega / c} \tag{9}$$

$v_a$  is easily proved to be virtually a linear function of  $v$  within a practical value of  $\omega$ . This means that the effect of projection inconsistency is negligible for flat terrain.

4.2 Case of Undulating Terrain

If the terrain is highly undulating, errors due to projection inconsistency are eliminated by correcting the focal length  $c$  at each image point. The error,  $\Delta v$ , is determined by Eq.10:

$$\Delta v = \Delta Z (\tan(\omega + \alpha) - \tan \omega) \cos \omega \tag{10}$$

where  $\Delta Z$  is the difference from ground level, as shown in Fig.1b. The error is proportional to  $\Delta Z$  and it can be eliminated by the following iterative procedure;

- 1) Assuming the terrain to be flat, the height  $Z$  is measured by bundle adjustment of the stereo observations based on Eqs.5. The resulting height will include a significant error at this stage.
- 2) The projection error is compensated by transforming  $p_a(v_a)$  to  $p'_a(v'_a)$  using Eqs.11 with the estimated value of  $\Delta Z$ :

$$c' = c + \Delta c, \quad \Delta c = \frac{\Delta Z}{\cos \omega}, \quad v' = \frac{vc'}{c}, \quad v'_a = \frac{v'}{1 - v' \tan \omega / c'} \tag{11}$$

- 3) The terrain height is again measured by bundle adjustment, this time using the updated affine image coordinates.
- 4) The above process, steps 1 to 3, is repeated until convergence. Experience suggests that even in quite mountainous terrain, only two or three iterations are needed.

4.3 Correction of Earth Curvature

If the 3D-GK coordinate system  $X, Y, Z$  and the local Cartesian coordinate system  $X_g, Y_g, Z_g$  are both set with their origins at the scene center, the difference in  $X_g$  and  $X$  or  $Y_g$  and  $Y$  will likely be negligible, but for  $Z$  and  $Z_g$  the difference will be appreciable as a result of Earth curvature. The height error at a ground point  $S$  km away from the origin is given by the well-known expression:

$$\Delta Z = Y^2 / 2R \text{ km} \tag{12}$$

where  $R = 6367$  km. This effect amounts to 67m in the margin of the SPOT scene used for the reported experiments. An alternative to compensation for Earth curvature is utilisation of Level 2 SPOT images, which are already free of projection errors. Otherwise the compensation can be imbedded into the process of image transformation from central perspective to affine projection.

## 5 EXPERIMENTAL TESTING

### 5.1 Orientation of a SPOT Stereo Scene

In order to evaluate the applicability of the affine projection model, as well as the other orientation models detailed above, a first series of tests were made using a SPOT stereo scene over western Japan (see also Okamoto et al., 1999 and Hasegawa et al., 1999). The two images are shown in Fig.2. These were recorded in November, 1996 (left) and in February, 1995 (right). The base-to-height (B/H) ratio of the image pair is a favourable 0.7. Two test sites were selected from the scene. One is a relatively small region called Kobe-AT (40km x 20km) which covers urban areas, seashore and mountains, with a maximum height difference of 800m. The other is a larger region called Kobe-Osaka (50km x 60km), which includes Kobe-AT. The maximum height difference in terrain in this broader region was again 800m.

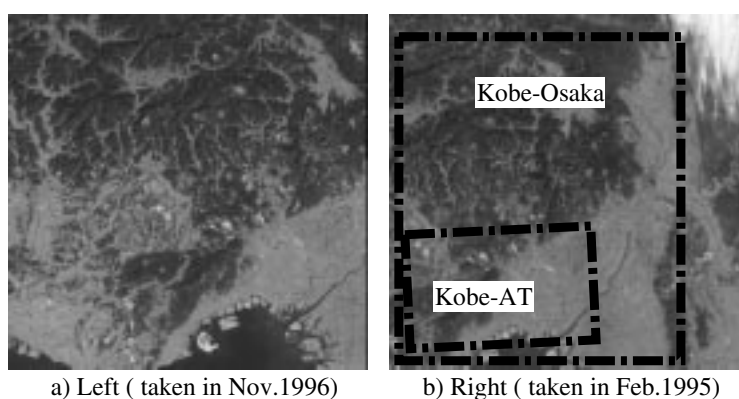


Figure 2: SPOT Images Used in Experiment

Orientation was conducted in the Japan Plane Orthogonal (JPO) coordinate system No.V, the projection system of which is Gauss-Krueger. GCPs and check points for orientation were prepared by aerial photogrammetry for Kobe-AT, and by photogrammetry and GPS surveying for Kobe-Osaka. Estimates of accuracy of GCPs are 0.3m in planimetry and 0.6m in height. In Kobe-AT, 117 points were utilised, while in Kobe-Osaka 48 ground points were employed. The heights employed were orthometric heights, though because of the minimal tilt of the geoid in the area, this aspect was of limited accuracy concern. Image coordinates were measured to 1/4 pixel accuracy by the digital stereo comparator, Kyoto-C (Ono et al., 1999).

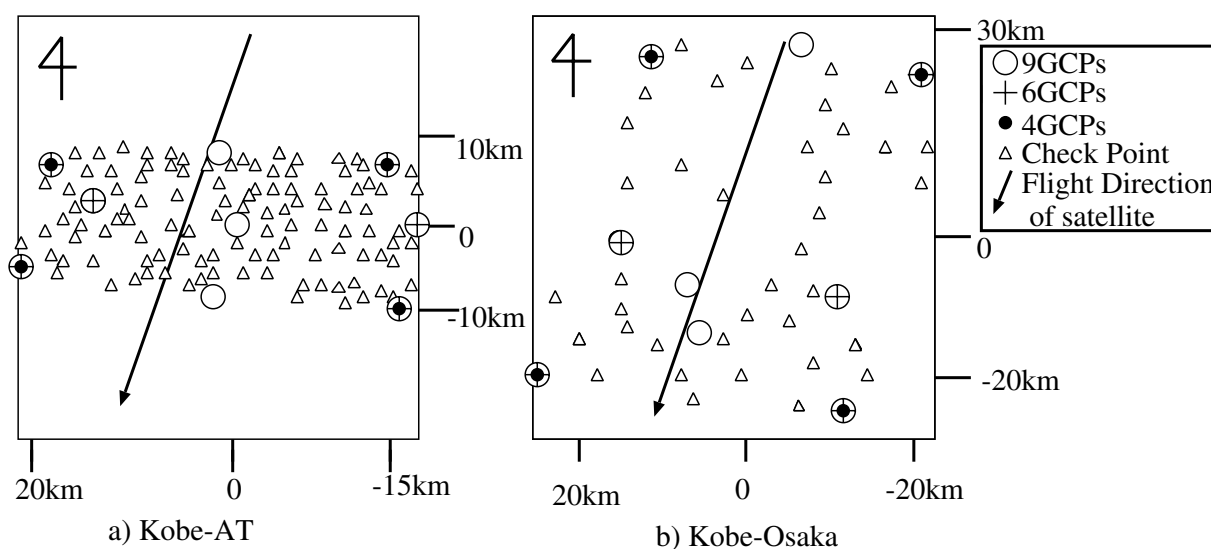


Figure 3: Disposition of GCPs and Check Points for Kobe-AT and Kobe-Osaka

Listed in Table 1 are the results obtained in the orientation/triangulation adjustments for Kobe-AT, based on four different models: 1D perspective model (Eqs. 2), the parallel perspective model (Eqs. 4), the 1D affine model (Eqs. 3) and the 2D affine model (Eqs. 5). Both internal and external measures of accuracy are listed. The internal precision (RMS 1-sigma) is obtained via the covariance matrix of parameters from the 'bundle adjustment', whereas the external accuracy is quantified through the RMS value of ground check point discrepancies. The time variation of parameters in the 1D perspective and 1D affine models was assumed to be linear. Fig.3a shows the disposition of GCPs and check points for Kobe-AT. Three patterns of control were tested, as indicated in Table 1 and Fig. 3a. These comprised four, six and nine GCPs. All other control points were used as check points.

With the exception of the case of the 1D perspective model with 4 GCPs, all models yielded sub-pixel external accuracies. Although there is little to distinguish the results of each algorithm, the 2D affine model produced the most consistently accurate ground point coordinates in the orientation/triangulation for the Kobe-AT test area.

Table 1: Orientation accuracy for Kobe-AT

model	4GCPs					6GCPs					9GCPs				
	$\sigma_0$ ( $\mu m$ )	internal accuracy		external accuracy		$\sigma_0$ ( $\mu m$ )	internal accuracy		external accuracy		$\sigma_0$ ( $\mu m$ )	internal accuracy		external accuracy	
		H	V	H	V		H	V	H	V		H	V	H	V
1p	4	3.4	10.7	5.7	13.5	3.9	3	8.9	5.3	7.4	4.1	2.8	8.3	5.1	6.4
pp	4	6.6	24.5	7.7	8.7	4	2.9	8.6	5.3	7.7	4	2.8	8.3	5.3	6.2
1a	3.8	3.3	8.9	5.8	6.9	3.8	2.8	7.9	5.5	6.6	3.9	2.7	7.8	5.2	6.2
2a	3.9	3	8.6	5.8	6.3	3.9	2.8	7.8	5.3	6.5	4	2.7	7.6	4.9	5.9

Unit of accuracy is meter

1p = 1D perspective model, pp = parallel perspective model, 1a = 1D affine model 2a = 2D affine model

The counterpart of Table 1 for Kobe-Osaka is Table 2, which confirms that the 2D affine model yields the optimum results. Not only did the 2D affine model produce the most accurate ground point coordinates, it proved to be the most stable algorithm. The accuracy discrepancy between Kobe-Osaka and Kobe-AT could be anticipated due to the differences in area, but a contribution also likely comes from limitations in the affine modelling over the larger image scene.

Table 2: Orientation accuracy for Kobe-Osaka

model	4GCPs					6GCPs					9GCPs				
	$\sigma_0$ ( $\mu m$ )	internal accuracy		external accuracy		$\sigma_0$ ( $\mu m$ )	internal accuracy		external accuracy		$\sigma_0$ ( $\mu m$ )	internal accuracy		external accuracy	
		H	V	H	V		H	V	H	V		H	V	H	V
1p	4.6	4.3	12.9	5.4	34.2	5.8	5.7	17.9	5.5	26.7	5.5	4.6	14.1	5.2	25
pp	5	6	19.8	8.8	19.8	5.6	5.9	18.2	8.6	10.1	4.9	4	10.9	5.5	9.4
1a	4	4	10.4	5.9	9.1	4.5	4.1	10.8	5.5	10.3	4.5	3.7	9.7	5.3	9
2a	4.7	4.4	11.8	7.1	10.3	4.5	3.7	9.8	6	9.5	4.8	3.6	9.7	5.6	8.7

### 5.2 Orientation of MOMS-2P images

The MOMS-2P 3-line stereo imaging sensor scans the ground in along-track mode, with the ground resolution of the forward- and backward-looking linear arrays of 2976 pixels being 18m x 18m and the sensor inclinations being +/-21.4°. The view angle is about seven degrees, which is significantly wider than SPOT. MOMS-2P operated from the MIR space station, which has an orbit height of about 400km and an orbit inclination of 51.6°. The stereo image pair used in the present experiment covered a 150km long, 50km wide strip over southeastern Germany and part of Austria. The maximum height difference in the underlying terrain was 180m. Some 58 GCPs were surveyed by GPS and Fig.4 shows their distribution. The orientation/triangulation adjustments, again utilising the same four mathematical models, were conducted in the UTM coordinate system. The resulting triangulation accuracies are shown in Table 4.

In the case of MOMS, the 1D and 2D affine models, along with the parallel projective model, display slightly better accuracy than the 1D projective model. For practical purposes, however, the accuracies produced by these three models can be considered equivalent. This is perhaps a consequence of the field view angle being a relatively wide 7°. Thus, the strength of the affine model does not show up.

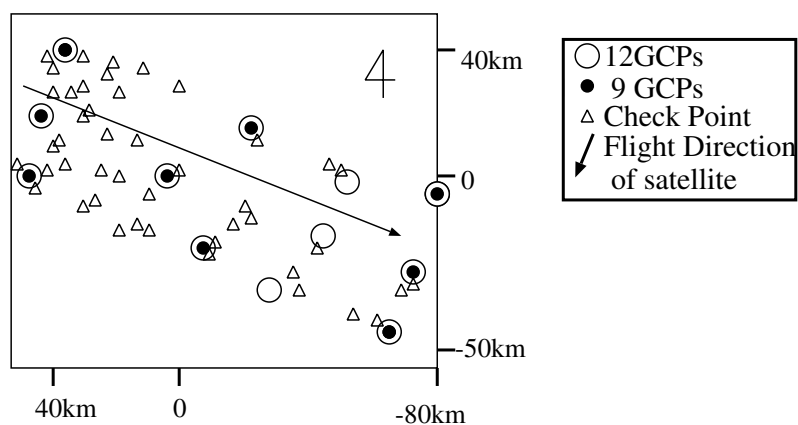


Figure 4: Disposition of GCPs and Check Points for MOMS-2P images

Table 3: Orientation result for MOMS-2P Image Pair

model	9GCPs					12GCPs				
	$\sigma_0$ ( $\mu\text{m}$ )	internal accuracy		external accuracy		$\sigma_0$ ( $\mu\text{m}$ )	internal accuracy		external accuracy	
		H	V	H	V		H	V	H	V
1p	2.3	10.8	13.1	14.2	14.3	2.3	9.3	11.4	12.4	10.6
pp	3.9	16	18.2	11.6	11.2	3.7	13.9	16.8	10.8	10.5
1a	2.4	10.7	14.4	11.8	12	2.4	8.8	12	11.1	10.3
2a	3.8	13.9	17.5	11.5	11.3	3.6	12.3	16.4	10.5	10.5

## 6 CONCLUDING REMARKS

The reported investigations have revealed the following properties of affine-based orientation/triangulation of satellite line scanner imagery:

- Affine projection is linear with regard to object point coordinates and thus closed-form orientation is possible. The inclination angle and the focal length are however necessary for image transformation from central perspective to affine projection.
- The precision of affine-based orientation corresponds well to that of central projection-based methods. As compared to the central projection models without exterior orientation constraints, the affine approach is generally more stable.
- The rank of affine-based observation equations is four, while that of central projection-based equivalents is seven. The degrees of freedom within a model formed by two overlapping affine images is 12 and the minimum number of required GCPs is four. On the other hand, the model created by two central perspective images has 15 degrees of freedom if interior orientation is treated as unknown, and the minimum required number of GCPs to orient the model is five. The burden of control surveying is, therefore, of little difference for the two orientation methods.
- Corrections to linear distortions in parameters( e.g. Earth rotation effect, uncertainty of geoid) are automatically incorporated in the affine observation equations.
- A major shortcoming of affine projection-based orientation is that the images taken with a sensor with a relatively wide field view angle, e.g. seven degrees for the MOMS-2P sensor, are not completely subject to affine geometry, but stand between affine and central projection. This produces measurement errors due to height differences and so these must be eliminated via iterative image transformations from central perspective to affine projection.
- The affine projection-based orientation needs to utilise either a local tangent plane XYZ coordinate reference system or a Gauss-Krueger projection coordinate system such as UTM; the model is not suited to earth centered coordinate systems since the satellite is assumed to fly in space at a constant velocity. Height errors due to earth curvature must of course also be compensated.

The above characteristics have been validated by the experiments conducted with the two satellite image pairs, one from SPOT (B/H ratio 0.75, maximum height difference of 800m) and one from MOMS-2P (B/H ratio 0.76, maximum height difference of 180m). For a range of different control point configurations, with a modest number of GCPs, the affine-based orientation produced ground point triangulation accuracies to sub-pixel level, namely about 0.5 to 0.7 pixels.

## REFERENCES

Gugan, D.J. and I.J. Dowman, 1988. Topographic Mapping from SPOT Imagery. PE&RS, Vol.54, No.10, October, pp.1409-1414.

Okamoto, A., Hasegawa, H., Fraser, C.S., Ono, T. and S. Hattori, 1999. Production of digital orthophotos from SPOT Imagery via an affine transformation Model. ASPRS Annual Conference, Portland, Oregon, May 17-21 (published on CD-ROM), pp.905-910.

Hofmann, O., 1986. Dynamische Photogrammetrie. Bildmessung und Luftbildwesen, Vol.54, Heft 5, pp.105-121.

Kratky, V., 1989. Rigorous Photogrammetric Processing of SPOT Images at CCM Canada. ISPRS Journal of Photogrammetry and Remote Sensing, 44: 53-71.

Konecny, G., Lohmann, P., Engel H. and E. Kruck, 1987. Evaluation of SPOT Imagery on Analytical Photogrammetric Instruments. PE&RS, Vol.53, No.9, September, pp.1223-1230.

Kruck, E. and P. Lohman, 1986. Aerial Triangulation of CCD Line-Scanner Images. ISPRS ComI. Symposium, Stuttgart, Sep 1986, 6pages.

Kruck, E., 1988. BINGO-SPOT, Restitution of SPOT Images, Gesellschaft fuer Industriephotogrammetrie mbH.

Okamoto A., 1981. Orientation and Construction of Models, Part III: Mathematical Basis of the Orientation Problem of One-Dimensional Central-Perspective Photographs. PE&RS, Vol.47, No.12, December, pp.1739-1752.

Okamoto, A., 1988. Orientation Theory of CCD Line-Scanner Images. International Archives of Photogrammetry and Remote Sensing (ISPRS), Vol.27, PartB3, Kyoto, pp.609-617.

Okamoto, A. and S. Akamatsu, 1992(a). Orientation Theory for Satellite CCD Line Scanner Imagery of Mountainous Terrain. ISPRS, Vol.29, PartB2, Washington, D.C., pp.205-209.

Okamoto, A. and S. Akamatsu, 1992(b). Orientation Theory for Satellite CCD Line Scanner Imagery of Hilly Terrain. ISPRS, Vol.29, Part B2, Washington, D.C., pp.217-221.

Okamoto, A., Hattori, S., Hasegawa H., and T. Ono, 1996. Orientation and Free Network Theory of Satellite CCD Line-Scanner Imagery. ISPRS, Vol.31, Part B3, Vienna, pp.604-610.

Okamoto, A., Fraser, C.S., Hattori, S., Hasegawa, H. and T. Ono 1998. An Alternative Approach to the Triangulation of SPOT Imagery. ISPRS, Vol.32, B4, Stuttgart, pp.457-462.

Okamoto, A., Ono, T., Akamatsu, S., Fraser, C.S., Hattori, S. and H. Hasegawa, 1999. The Geometric Characteristics of Six Alternative Triangulation Models for Satellite Imagery. ASPRS Annual Conference, Portland, Oregon, May 17-21 (published on CD-ROM), pp.64-72.

Ono, T., Hattori, S., and H. Hasegawa, 1999. Digital Stereo Plotter for High Resolution Satellite Imagery. ISPRS Com V/SIG Animation, Int. Workshop on Vision-Based Technical in Visualization and Animation, Onuma, Oct 14-16, pp.191-194.

Trinder, J.C., Donnelly, B.E. and Kwoh Leong Keong, 1988. SPOT Mapping Software for WILD Avilyt BC2 Analytical plotter. Proc. Of IGRASS'88 Symposium, Edinburgh, Scotland, 13-16 Sept, pp.1801-1806.

Westin, T., 1990. Precision Rectification of SPOT Imagery. PE&RS, Vol.56, No.2, February, pp.247-257.